Contents lists available at ScienceDirect

Journal of Membrane Science

journal homepage: www.elsevier.com

Transformation of cross-linked polyimide UF membranes into highly permeable SRNF membranes via solvent annealing

Hanne Mariën, Ivo F.J. Vankelecom*

Centre for Surface Chemistry and Catalysis, KU Leuven, Celestijnenlaan 200f, PO 2461, 3001 Leuven, Belgium

ARTICLE INFO

Keywords:
Solvent-resistant nanofiltration
Solvent annealing
Densification
Cross-linked polyimide

ABSTRACT

A simple method for the preparation of highly permeable solvent-resistant nanofiltration (SRNF) membranes was developed. By applying a solvent treatment to cross-linked polyimide ultrafiltration membranes, polymer chain flexibility increased and the matrix rearranged into a more dense structure, creating highly selective SRNF membranes with exceedingly high ethanol permeance. This densification was driven by the ability of the membrane to lower its free energy while in the solvated state via the establishment of extra favorable interactions, like hydrogen bonds and π interactions. Moreover, further reaction of only partly reacted cross-linker molecules was completed during the treatment, thus enhancing the cross-linking degree. The extent of densification depended on the type of solvent, the immersion time and the initial cross-linking degree of the membrane, all influencing the degree of solvation and chain rearrangement. By altering the synthesis conditions, a membrane with equal selectivity to Duramem 300 but showing a 400% higher ethanol permeance was obtained. This demonstrates the high potential of the technique to be applied as novel method for the preparation of SRNF membranes with exceptionally high solvent permeance.

1. Introduction

Nanofiltration (NF) is a pressure-driven membrane process in which low molecular weight components (< 1000 Da) can be retained. This technique is widely applied in aqueous separation processes, e.g. for the removal of dissolved organic matter, pesticides, disinfection by-products, divalent ions, heavy metals and pharmaceuticals from surface water, groundwater and wastewater [1–3]. More recently, solvent resistant nanofiltration (SRNF) has emerged as a potential energy-saving replacement for distillation and a waste-free alternative for extractions and chromatographic separations in the (petro)chemical, pharmaceutical and food industry [4–6]. Since 40–70% of the capital and operating costs in the chemical and pharmaceutical industry are related to separation processes [7], improvements in this field can contribute significantly to the creation of a cost-efficient production process. Moreover, the ambient temperature conditions of SRNF allow the separation of mixtures containing thermolabile components, in contrast to distillation.

Since SRNF can be a valuable separation technique in several industrial processes, potential applications have been intensively investigated [5]. Real industrial SRNF applications are however still scarce. This is largely caused by the conditions of solvent stability, high solvent permeance and high solute retention which all must be satisfied. Moreover, the wide range of organic solvents applied in industry makes the membrane performance and stability strongly depending on the application. Most SRNF membranes are integrally skinned asymmetric (ISA) membranes, which can be cross-linked to enhance their solvent stability [8–11]. Due to the rather low permeance of many organic solvents through these types of membranes, the use of thin-film composite (TFC) membranes, with a selective layer of less than 100 nm thick, is being investigated nowadays [12–16]. The most common type of TFC membranes are interfacially polymerized polyamide membranes, which are widely applied in aqueous NF and reverse osmosis applications [17]. Although the water permeance is high due to the hydrophilicity of the selective layer, the permeance of many (more apolar) organic solvents is still too low to be applied in industry [18]. An improvement in organic solvent permeance of either ISA or TFC membranes could therefore greatly contribute to the large-scale implementation of SRNF.

A new, easy method is presented here to prepare ISA SRNF membranes with a strikingly improved solvent permeance. In this method,

* Corresponding author.
Email addresses: hanne.marien@kuleuven.be (H. Mariën); ivo.vankelecom@kuleuven.be (I.F.J. Vankelecom)

http://dx.doi.org/10.1016/j.memsci.2017.06.080
Received 9 May 2017; Received in revised form 26 June 2017; Accepted 28 June 2017
Available online xxx
0376-7388/

polyimide-based ultrafiltration (UF) membranes, having a generally thinner skin layer than ISA NF membranes, were first prepared via phase inversion. Then, the thin skin layer of the cross-linked membrane was selectively densified by performing a solvent treatment to rearrange the polymer chains. By comparing the resulting SRNF membranes with commercial SRNF membranes with equal selectivity, a 400% improvement in ethanol permeance was proven. Moreover, a 184% improvement in ethanol permeance compared to state-of-the-art lab-prepared TFC membranes with similar selectivity [19], generally showing a higher permeance than ISA membranes, was observed.

2. Experimental

2.1. Materials

Polyimide (PI, Matrimid® 9725) was purchased from Huntsman (Switzerland). The non-woven polypropylene/polyethylene (PP/PE) fabric Novatexx 2471 was kindly provided by Freudenberg (Germany). Hexanediamine (HDA, 99.5%, Acros) was used for membrane cross-linking. N-methylpyrrolidone (NMP, 99%, Acros), tetrahydrofuran (THF, 99.9+%, Sigma-Aldrich), n-hexane (99+%, Chem-Lab), acetonitrile (ACN, 99.99%, Fisher), dimethylformamide (DMF, 99+%, Acros), ethanol (EtOH, 99.99%, Fisher) and 1-butyl-3-methylimidazolium bis(trifluoromethylsulfonyl)imide ([C_4mim][Tf_2N], 99+%, Iolitec) were used as received. Rose Bengal (RB, 1017 Da, Sigma Aldrich, Figure A.1 in appendix A) and methyl orange (MO, 327 Da, Fluka, Figure A.1 in appendix A) were used as test solute.

2.2. Membrane synthesis

UF membranes were synthesized via phase inversion. PI powder was first dried overnight in an oven at 100 °C. Homogeneous polymer solutions were prepared by stirring mixtures of PI (14% (w w^{-1})) in NMP/THF (75/25). They were left untouched overnight to remove air bubbles created during the stirring. The polymer solution was cast at a constant speed (4.4 10^{-2} m s^{-1}) and with a wet thickness of 200 μm using an automatic casting device (Braive Instruments, Belgium) on a PP/PE non-woven impregnated with NMP. After a 30 s evaporation to allow THF evaporation from the surface, the film was immersed in a coagulation bath. The coagulation bath consisted of HDA (0.5% (w v^{-1})) in Milli-Q water to simultaneously perform phase inversion and cross-linking of the membrane [13,20,21]. After 5 min, the membrane was removed from the coagulation bath and stored in water until further use. In specified cases where a more dense membrane was desired, a polymer concentration of 16% (w w^{-1}), an NMP/THF ratio of 70/30 or 60/40 or an evaporation time of 60 s was applied. In other specified cases, a HDA concentration of 2.0% (w v^{-1}) and an immersion time in the coagulation bath of 60 min were used to form more strongly cross-linked membranes.

After synthesis and storage of the membranes in water, the cross-linked PI membranes were immersed in a solvent (hexane, EtOH, ACN, [C_4mim][Tf_2N] or DMF) for specified times (1 min, 1.5 h, 30 h or 70 h). Afterwards, they were stored in water for at least 16 h until filtration.

2.3. Membrane performance

A high-throughput filtration module which allows to run 16 simultaneous dead-end filtrations under exactly the same operating conditions was used to test the membrane performance [22]. The active area of each membrane coupon was 1.54×10^{-4} m^2. To minimize concentration polarization, the feed was stirred at 400 rpm. The membrane performance was evaluated with a RB or MO solution in EtOH (both 35 μM). Four coupons per membrane were tested simultaneously and the performance was averaged.

The permeance P (L m^{-2} h^{-1} bar^{-1}) was calculated using Eq. (1), with V (L) the permeate volume, A (m^2) the membrane area, t (h) the filtration time and ΔP (bar) the applied pressure:

$$P = \frac{V}{A \times t \times \Delta P} \quad (1)$$

The retention R (%) was calculated using Eq. (2), with c_f and c_p the solute concentration in feed and permeate respectively:

$$R = \frac{c_f - c_p}{c_f} \times 100 \quad (2)$$

RB and MO concentrations in EtOH were determined with a UV–Vis spectrophotometer (UV-1650 PC, Shimadzu) at 550 and 416 nm respectively.

2.4. Characterization

Membrane cross-sections were analyzed with scanning electron microscopy (SEM), using a JEOL JSM-6010LV SEM. Before the measurement, a conductive gold/palladium layer was deposited on the samples with a JEOL JFC-1300 auto fine coater.

To analyze skin layer cross-sections at high resolution, transmission electron microscopy (TEM) was applied. Unstained membrane samples were embedded in an araldite resin (Polyscience) and cut into ultrathin (70 nm) cross-sections with a Reichert Ultracut E microtome. Images were taken with a JEOL ARM-200F at 80 kV.

The roughness of the membrane surface was analyzed with atomic force microscopy (AFM) at ambient conditions using an Agilent 5500 AFM in tapping mode with NCSHR probes from NanoAndMore GmbH. The cantilever was made out of Si with a spring constant of 40–50 N m^{-1} and a nominal tip apex radius of < 5 nm. On each sample, three positions with an area of 25 μm^2 were scanned and analyzed with the WSxM software [23]. The reported root-mean square (RMS) roughness is the average of three different positions of 6.25 μm^2 on the same sample.

Attenuated total reflectance infra-red (ATR-IR) spectroscopy was used to determine the chemical composition of the membrane surface after drying, taking 64 scans at a resolution of 4 cm^{-1} with a Varian 620 FT-IR imaging microscope with a germanium crystal.

The change in free volume in the membrane skin layer was analyzed using the pulsed low energy positron system (PLEPS) at the neutron induced positron source Munich (NEPOMUC). The measurements were performed at ambient temperature (30 °C) with implantation energies of 0.5–4.0 keV. The pick-off lifetime of the o-positronium, which can be extracted from the measured spectra, was correlated to the free volume hole size using the Tao-Eldup model [24,25].

To determine the weight loss of the membrane after immersion in a solvent, a dry piece of membrane (without non-woven) was weighed before and after immersion. The membrane was dried in an oven at 80 °C for at least 24 h. After immersion in a non-volatile solvent, the membrane was washed with water before drying. The weight loss was calculated using Eq. (3), with m_i and m_f (g) the initial and final dry mass of the membrane piece respectively.

$$Weight\ loss = \frac{m_i - m_f}{m_i} \times 100 \quad (3)$$

To determine the degree of swelling of the membrane during immersion in a solvent, a dry piece of membrane (without non-woven) was first impregnated with water and, after drying, impregnated with the solvent. As the membrane does not swell in water, its pore volume

can be derived from the wet mass after impregnation with water. The extra volume of solvent taken up in the polymer matrix is then related to the degree of swelling. It was calculated using Eq. (4), with m_m, m_{m+s} and m_{m+w} (g) the mass of the dry membrane, and the solvent or water impregnated membrane respectively, and ρ_s and ρ_w the density of the solvent and water respectively.

$$Degree\ ofswelling = \frac{\frac{m_{m+s}-m_m}{\rho_s} - \frac{m_{m+w}-m_m}{\rho_w}}{m_m} \quad (4)$$

2.5. Interaction parameters

The difference in Hansen solubility parameters between the uncross-linked PI membrane and the solvents used for immersion ($\Delta_{solvent\text{-}PI}$) was calculated using Eq. (5) [26], with δ_D, δ_P and δ_H the contribution of dispersive interactions, polar bonding and hydrogen bonding, respectively. A low $\Delta_{solvent\text{-}PI}$ indicates a strong interaction between the membrane and the solvent.

$$\Delta_{solvent-PI} = \sqrt{4(\delta_{D,solvent} - \delta_{D,PI})^2 + (\delta_{P,solvent} - \delta_{P,PI})^2 + (\delta_{H,solvent} - \delta_{}$$

3. Results

3.1. Principle

Membranes with a dense skin layer with selectivities in the NF range were formed by preparing cross-linked PI UF membranes via phase inversion, followed by a solvent treatment. The solvent treatment caused (the skin of) the membrane to densify, drastically improving the selectivity of the membrane. The extent of this effect depended on the type of solvent, the immersion time and the cross-linking degree of the membrane, as discussed in 3.2, 3.3 and 3.4. Under the optimal conditions, a UF membrane could be transformed into a highly selective NF membrane with a superior performance compared to commercial SRNF membranes (directly prepared via phase inversion), as presented in 3.5.

The principle of the solvent treatment is presented in Fig. 1. After casting the PI solution into a thin film, the highly solvated, flexible polymer chains are in a disordered state to minimize their free energy. During phase inversion, the film is transformed into a solid membrane. Because this demixing process occurs instantaneously, the polymer chains are 'frozen' in their initial, disordered conformation, without reaching the thermodynamic equilibrium. By adding HDA to the coagulation bath, the membrane is cross-linked during phase inversion, making it resistant to dissolution in any organic solvent, and 'fixing' the non-equilibrium state even more effectively. When the membrane is then immersed in a good solvent for the polymer, the interaction between the solvent and the membrane causes re-solvation of the polymer chains, thus increasing their mobility. This improved flexibility is expected to enable the PI chains to reorganize and establish extra favorable interchain interactions, like π interactions between the aromatic rings and hydrogen bonds, resulting in a decrease in free energy. Moreover, partly unreacted HDA molecules can at that moment better approach imide groups in the surrounding, flexible PI chains which were not yet cross-linked before, leading to extra cross-linking. This reorganization and the resulting interactions and cross-linking between the polymer chains are expected to lower the interchain distance and create a more dense membrane. Since the membrane is asymmetric, having a more dense skin on top of a highly porous sublayer, the largest effect is assumed to be observed in the skin layer, where the polymer chains are already in close proximity before the solvent treatment. Further densification of the skin layer can then cause the membrane to be transformed from a UF to a NF membrane.

It is thus expected that the effect on chain flexibility and subsequent membrane densification in the case of solvation of the polymer chains during immersion in a good solvent, as described in this work, is sim-

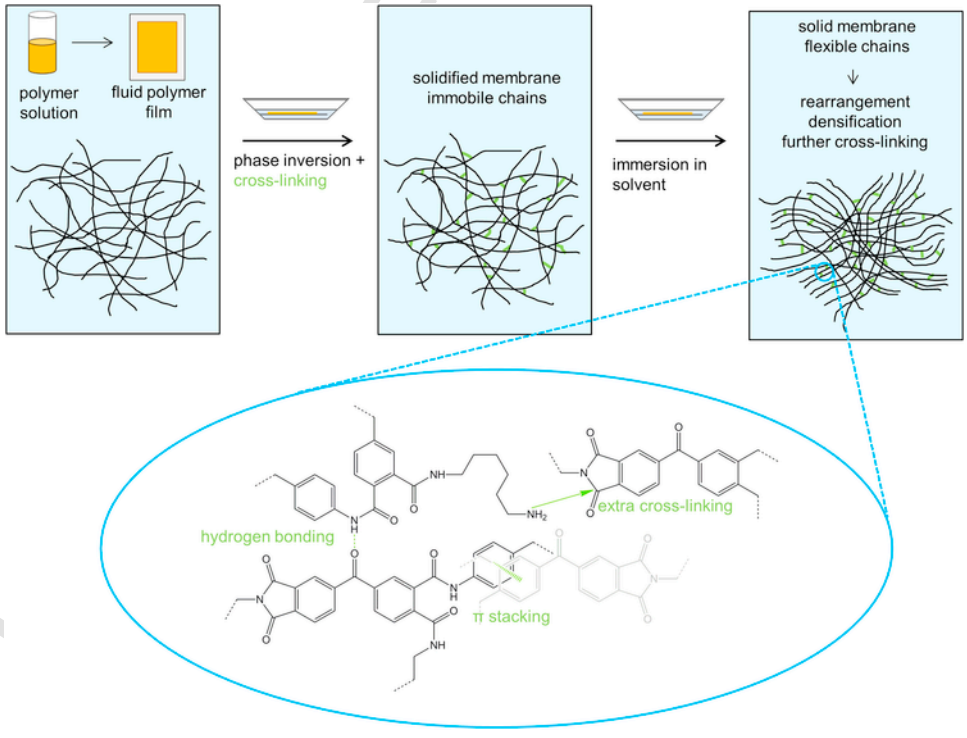

Fig. 1. Basic principle of the post-synthesis membrane densification via solvent treatment.

ilar to the effect of applying high temperature annealing, as often accomplished in e.g. gas separation, aqueous NF or SRNF [27–31]. During high temperature annealing, the increased temperature is also assumed to cause a thermodynamically driven reorganization of the polymer chains towards more dense structures [32].

3.2. Solvent type

First, the effect of a 30 h immersion of cross-linked PI membranes in different types of solvents was investigated. Because ionic liquids are an emerging class of solvents in polymer synthesis [33,34], and more specifically in membrane preparation [19,35,36], [C_4mim][Tf_2N] was incorporated in the study as an example of this type of solvents. The results are shown in Fig. 2. Without solvent treatment, the membrane showed a very low RB retention, together with a high EtOH permeance, as could be expected from a membrane prepared using a typical UF membrane recipe. All tested solvents caused the retention to increase and the permeance to decrease, but to an extremely different extent. While the effect of immersing the membrane in hexane, EtOH and ACN was low to moderate, a very strong effect was observed after immersion in [C_4mim][Tf_2N] and DMF. Pictures of the membrane coupons after filtration (Fig. 2) clearly prove that – in clear contrast to the four other samples – no RB was sorbed in the membranes treated with [C_4mim][Tf_2N] and DMF, indicating that the increased retention is not realized by dye adsorption on or in the membrane, but that a true densification of the skin had occurred.

A washing step with water of at least 16 h was applied between the solvent treatment and the filtration, during which EtOH, ACN and DMF were removed. Hexane and [C_4mim][Tf_2N], however, are immiscible with water, and could thus still have been present in the membrane at the start of the filtration, during which they were removed by EtOH. The observed decrease in permeance over time of the membrane treated with [C_4mim][Tf_2N] might indicate that the polymer chains were still somewhat solvated and flexible at the start of the filtration, caused by the initial presence of residual ionic liquid.

To link the densification effect of the different solvents to membrane-solvent interactions, which would cause solvation and reorganization of the flexible polymer chains, the difference in Hansen solubility parameters between PI and the different solvents ($\Delta_{s\text{-}p}$) was calculated (Table A.1 in appendix A). $\Delta_{water\text{-}p}$ was also included, since the performance of the reference membrane without solvent treatment corresponds to a membrane stored in water before filtration. Only $\Delta_{[C4mim][Tf2N]\text{-}p}$ could not be calculated because the Hansen solubility parameters are not available for this solvent.

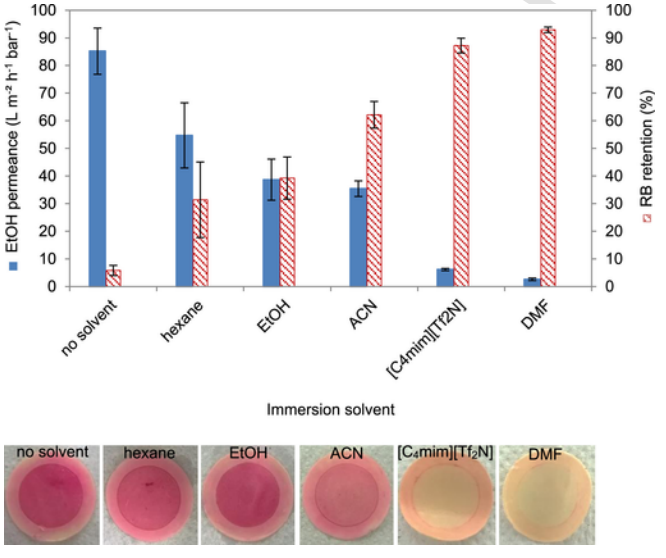

Fig. 2. EtOH permeance and RB retention of cross-linked PI membranes after 30 h of immersion in different solvent types (top) and visual observation of possible sorption of RB in the membrane coupons during the filtration (bottom).

Fig. 3 shows the decrease in permeance and increase in retention caused by the solvent treatment, as function of the difference in Hansen solubility parameters between the membrane and the solvent used for the treatment. The trend indicates that the solvents having the smallest effect on membrane performance (lowest $\Delta_{EtOH\ permeance}$ and $\Delta_{RB\ retention}$) also had the weakest interaction with the PI membrane (highest $\Delta_{s\text{-}p}$), while the interaction increased for solvents having a larger effect on membrane performance. This supports the hypothesis of the need for sufficient swelling to reorganize the polymer chains. The larger densification effect of EtOH compared to hexane (Fig. 2), which contradicts their equal $\Delta_{s\text{-}p}$ values in Table A.1 in appendix A, can be explained by the fact that these values were calculated using the Hansen solubility parameters of pristine, non-cross-linked PI. Cross-linking the PI membrane caused the polarity of the membrane to increase, improving its interaction with EtOH, while diminishing its affinity for hexane.

As the magnitude of the membrane-solvent interaction changes with the type of solvent, a difference in swelling behavior of the membrane should also be observed. Therefore, the degrees of swelling and the weight losses of the membrane after a 30 h immersion in the different solvents were calculated. The weight loss was expected to be proportional to the degree of swelling, since a larger membrane-solvent interaction would both cause a larger swelling and a higher solubility, hence facilitating leaching of non-cross-linked polymer chains from the membrane. The degree of swelling could only be measured accurately in the case of non-volatile solvents, while the weight loss could only be determined when the solvent was able to evaporate or to be fully replaced by water, which could then be evaporated.

As shown in Fig. 4a, hexane and EtOH, having the highest $\Delta_{s\text{-}p}$, did not induce any significant weight loss of the membrane. However, the weight loss increased after immersing the membrane in ACN and, even more, in DMF, corresponding to the trend in $\Delta_{s\text{-}p}$. The differences in weight loss perfectly agree with the trend in membrane performance, as elucidated in Fig. 4b. It should be mentioned that the weight loss remained low (< 6%) for all membranes, suggesting that the membrane integrity was maintained. A too high weight loss could result in a loss of membrane structure and performance. Also the swelling degree of the membrane increased going from [C_4mim][Tf_2N] to DMF as immersion solvent (Fig. 4a).

Densification was expected to be caused by both the establishment of favorable interactions between the polymer chains and by further cross-linking of the PI matrix (Fig. 1). The effect of the solvent treat-

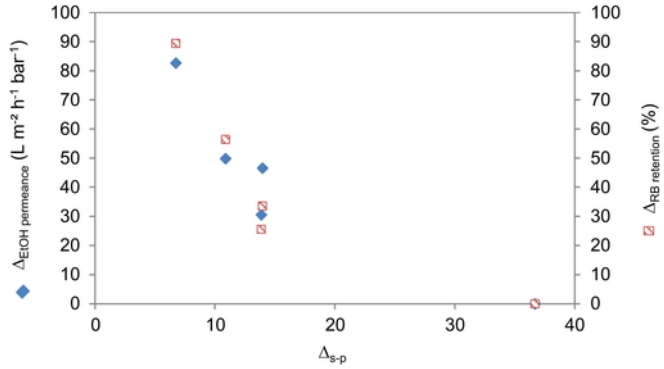

Fig. 3. Change in EtOH permeance and RB retention of cross-linked PI membranes caused by the solvent treatment, as function of their interaction with the respective solvents used for the treatment.

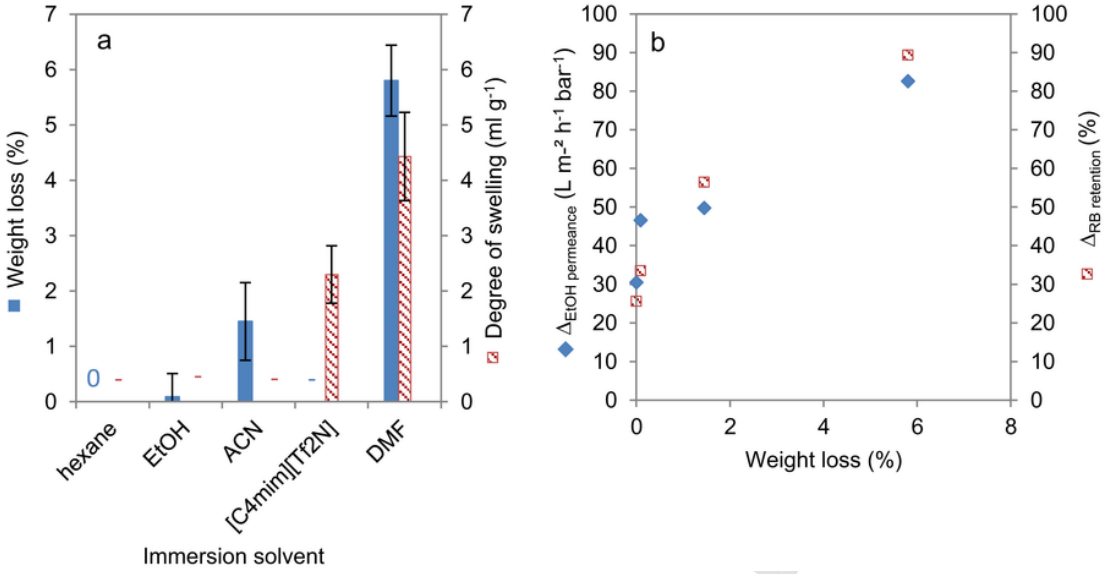

Fig. 4. (a) Weight loss and degree of swelling of cross-linked PI membranes after 30 h of immersion in different solvent types. '0' means the value was zero, '-' means the value was not measured. (b) Change in EtOH permeance and RB retention of cross-linked PI membranes caused by the solvent treatment, as function of their weight loss after immersion in the respective solvents.

ment on the degree of cross-linking of the membranes is shown in Fig. 5. To quantify the cross-linking degree, the ratio of the amide over imide absorbance was calculated, since cross-linking causes the imide bonds of the PI membrane to be transformed into amide bonds. A higher amide/imide ratio thus indicates a stronger cross-linking. The largest imide (at 1720 cm^{-1}) and amide signals (at 1602 and 1662 cm^{-1}) in the UV–vis spectrum were used to calculate the ratio. Fig. 5 indicates that the cross-linking degree of the membranes did not change significantly after immersion in hexane, EtOH and ACN. Immersion in [C_4mim][Tf_2N] and DMF, however, caused the membranes to be further cross-linked. Especially when using DMF, the difference in cross-linking degree with the reference membrane was large. This proves that during the initial phase inversion and cross-linking step, not all HDA molecules are able to react at both sides with a PI chain, probably because the PI chains are 'frozen' instantaneously when immersing the polymer film in the coagulation bath containing the cross-linker. Subsequent immersion of the solidified membrane in a solvent which makes the polymer matrix swell significantly ([C_4mim][Tf_2N] or DMF), causes the PI chains to become flexible, and enables the unreacted amine group of HDA to physically reach a second polymer chain to complete its cross-linking reaction. This improvement of membrane cross-linking is assumed to be one of the driving forces of the densification of the membrane.

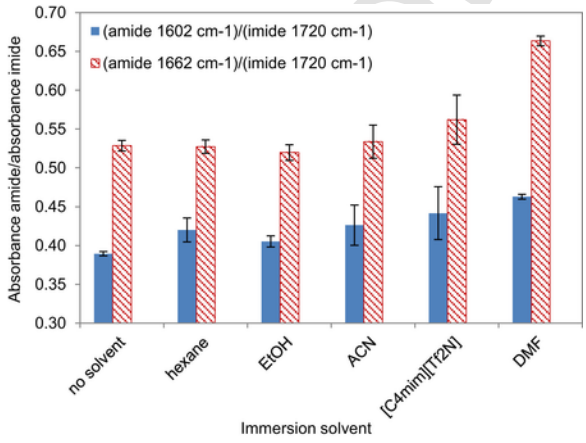

Fig. 5. ATR-IR results of cross-linked PI membranes after 30 h of immersion in different solvent types. The amide/imide absorbance ratio indicates the cross-linking degree of the membranes.

In an attempt to visualize the change in membrane density and pore structure caused by immersion in the different solvents, SEM and TEM cross-sectional images were made. The SEM images in Fig. 6a, b and c indicate that the overall membrane pore structure was not altered by the solvent treatments. By focusing on the skin layer of the membrane with TEM, an increase in thickness of the denser layer was observed after treating the membrane with ACN or DMF (Fig. 6d, e and f). However, the difference was small and difficult to quantify. It is therefore expected that the density (free volume) of the skin layer rather than its thickness is affected by the solvent treatment. An attempt was made to quantify this change in free volume with PLEPS. However, since o-Positronium formation is inhibited in some materials, like polyimide [37], extremely low intensities were measured and the results were not useful.

Also the surface morphology was assumed to be affected by the solvent treatment. Reorganization of the polymer chains into a more densely packed structure was expected to lower the surface roughness. AFM indicated that the RMS roughness indeed decreased from 5.2 (± 0.6) nm for the reference membrane to 4.2 (± 0.4) nm or 3.6 (± 0.2) nm after immersion in ACN or DMF respectively (Fig. 6g, h and i), which corresponds to the expected extent of reorganization in polymer chains caused by these two solvents.

3.3. Immersion time

Since DMF had the largest effect on membrane performance, this solvent was chosen to investigate the influence of the immersion time. As shown in Fig. 7a, a 1 min immersion in DMF already caused the RB retention to increase drastically towards the NF range, while the permeance dropped accordingly. By increasing the immersion time to 1.5 h, the effect on performance was intensified. However, a further increase of the immersion time resulted in a small reversal of the densification effect.

To explain this trend, the swelling degree and weight loss of the membranes after different immersion times was determined (Fig. 7b). Although swelling occurs immediately after immersion and the

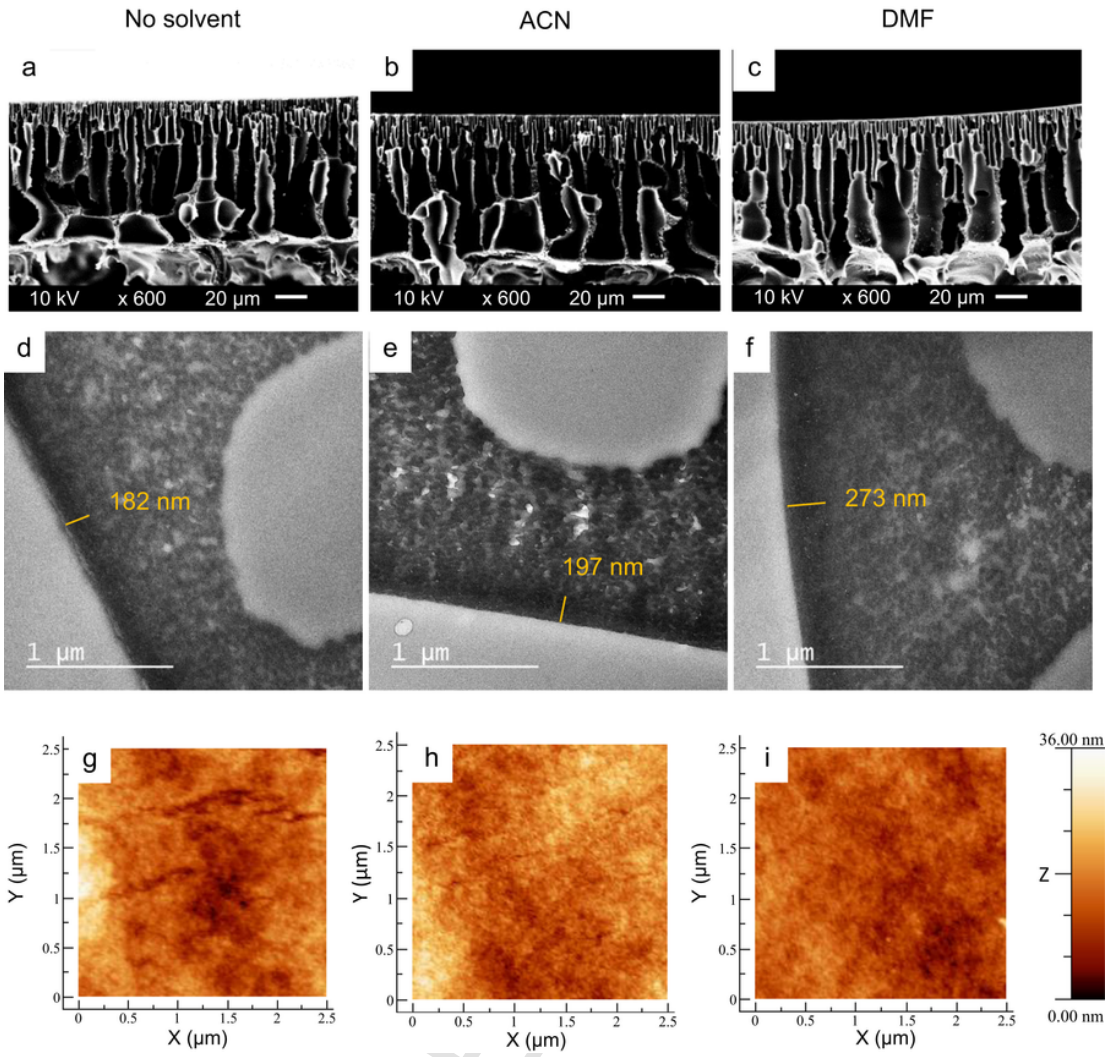

Fig. 6. (a, b, c) Cross-section SEM images, (d, e, f) cross-section TEM images and (g, h, i) surface AFM images of cross-linked PI membranes without solvent treatment or after 30 h of immersion in ACN or DMF.

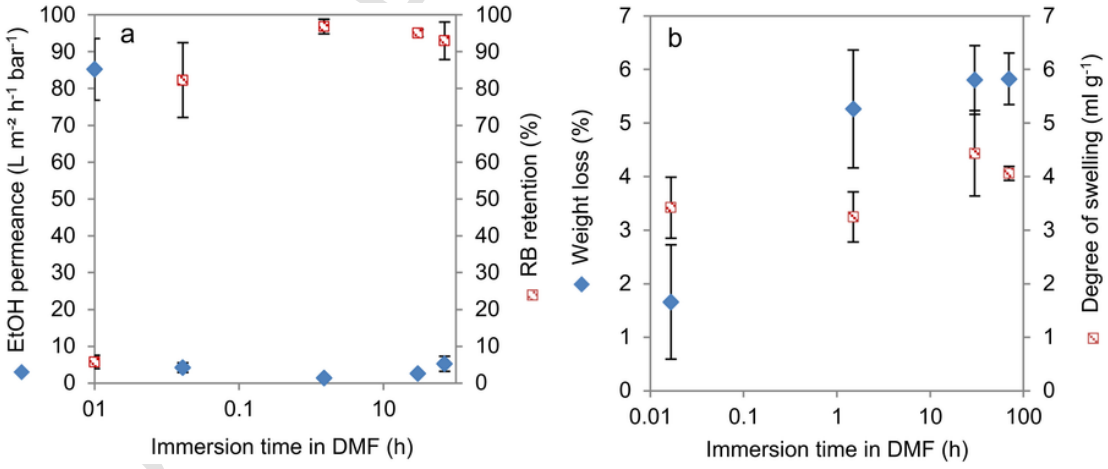

Fig. 7. (a) EtOH permeance and RB retention of cross-linked PI membranes after immersion in DMF for different times (log scale), and (b) weight loss and degree of swelling of cross-linked PI membranes after immersion in DMF for different times (log scale).

swelling degree remains constant at increasing immersion times, 1 min is probably too short for the polymer chains to fully rearrange and establish interchain interactions and cross-linking. Therefore, a further increase in RB retention and decrease in EtOH permeance takes place at longer treatment times (Fig. 7a). The weight loss however, is still very small after 1 min immersion due to the rather slow disentanglement and leaching of non-cross-linked PI chains. The increasing weight loss after longer DMF treatments possibly counteracts the mem-

brane densification effect, which might explain the slightly reversing trend in performance after 30 and 70 h immersion (Fig. 7a).

3.4. Degree of cross-linking

Since cross-linking limits the PI chains to become flexible and rearrange during immersion in a solvent, membranes with a higher degree of cross-linking after the coagulation step were expected to be less affected by the solvent treatment. Therefore, more strongly cross-linked PI membranes were prepared and the effect of immersion in [C_4mim][Tf_2N] and DMF on their performance was investigated. First, the significant difference in cross-linking between the two membranes, realized by altering the HDA concentration and reaction time, was demonstrated with ATR-IR (Fig. 8). The strongly cross-linked PI membrane (high-XL) clearly shows larger amide signals (green bars) and reduced imide signals (blue bars). The spectrum of an uncross-linked PI membrane is shown for comparison.

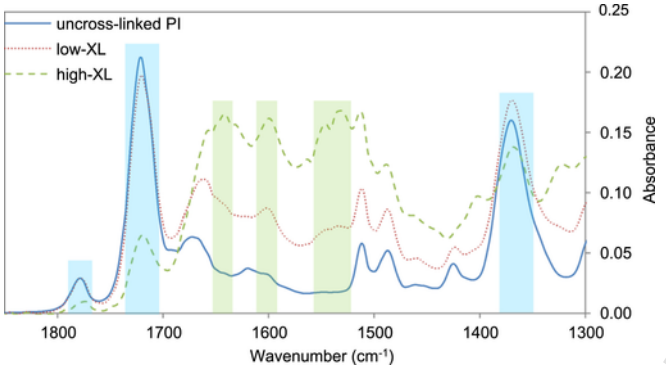

Fig. 8. ATR-IR spectra of PI membranes with a low (low-XL) and high degree of cross-linking (high-XL), and an uncross-linked PI membrane for comparison. The blue bars represent imide and the green bars amide signals. (For interpretation of the references to color in this figure legend, the reader is referred to the web version of this article)

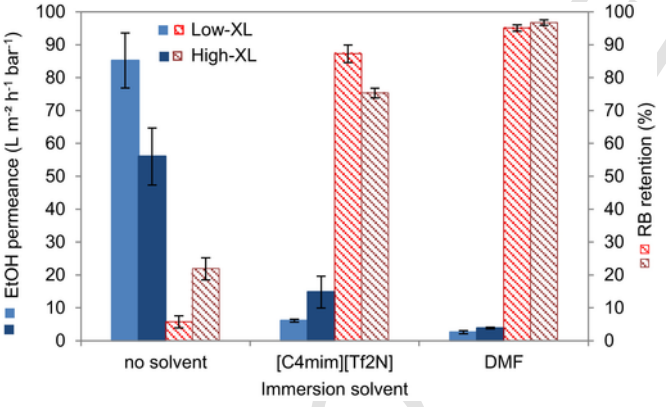

Fig. 9. EtOH permeance and RB retention of PI membranes with low (low-XL) and high degree of cross-linking (high-XL), before and after immersion in [C_4mim][Tf_2N] and DMF for 30 h.

As shown in Fig. 9, increasing the cross-linking degree of the membrane (without solvent treatment) caused the membrane to densify, as derived from the decreasing EtOH permeance and increasing RB retention. However, after immersion in [C_4mim][Tf_2N] or DMF, the increase in retention and decrease in permeance (relative to the value of the non-treated membranes) was lower at higher cross-linking degree. This difference was more pronounced for [C_4mim][Tf_2N] than for DMF. Increasing the cross-linking thus clearly lowered the effect of the solvent treatment. This can either be caused by the lower potential of a more highly cross-linked membrane to reorganize, or by the lower diffusion rate of the solvents inside a more dense, highly cross-linked membrane, reducing the available time for reorganization.

3.5. Formation of nanofiltration membranes

NF membranes are classified as membranes having a MWCO of less than 1000 Da [38]. RB has a MW of 1017 Da and therefore represents the upper limit of NF. The best performing membrane prepared by the solvent treatment, showed a RB retention of 96.8% and an EtOH permeance of 1.44 L m^{-2} h^{-1} bar^{-1} (Figs. 7a, 1.5 h immersion in DMF) and can thus be classified as a NF membrane. It was however expected that even more dense membranes could be prepared by changing the synthesis conditions, which could then be transformed again into even tighter NF membranes by applying the solvent treatment.

Table 1 shows the synthesis conditions of cross-linked PI membranes in which either polymer concentration, NMP/THF ratio or evaporation time were adapted to obtain denser membranes. For every membrane, a 1.5 h DMF treatment was applied after phase inversion, and membrane performance was determined with a solution of MO in EtOH. This dye (MW = 327 Da) was more suitable than RB to distinguish the selectivities of these denser membranes. As derived from Fig. 10, an increase in polymer concentration form 14–16% (w w^{-1}) or a decrease in NMP/THF ratio from 70/30 to 60/40 both resulted in an improved selectivity without loss in permeance. An increase in evaporation time, however, caused the permeance to decrease significantly, probably by increasing the thickness of the skin layer [28,39,40]. Combining the higher polymer concentration and lower NMP/THF ratio resulted in a highly selective NF membrane with a 95% MO retention, while the EtOH permeance remained unaffected (i.e. 1.1 L m^{-2} h^{-1} bar^{-1}).

In Fig. 11, the performance of Duramem 500 and Duramem 300 (commercial, cross-linked PI membranes) is compared with the solvent treated membranes prepared in this work. Membranes from Fig. 10 with a selectivity similar to the Duramem membranes were selected to compare the EtOH permeance more correctly. Since Duramem 500 has a MWCO of 500 Da, it showed a MO retention below 90%. The solvent treated PI membrane with similar selectivity had a significantly higher EtOH permeance (× 270%). The more dense Duramem 300 showed a higher MO retention and, accordingly, a lower EtOH permeance. In this case, an even larger difference in EtOH permeance could be observed (× 400%). The DMF treatment of cross-linked PI-based UF membranes thus clearly proved to result in high-performance NF membranes with

Table 1
Conditions for the preparation of denser, cross-linked PI membranes (with low cross-linking degree) via phase inversion, followed by a DMF treatment.

Membrane	PI concentration (% w w^{-1})	NMP/THF ratio (w w^{-1})	Evaporation time (s)	Immersion time in DMF (h)
PI-ref	14	70/30	30	1.5
PI-16%	**16**	70/30	30	1.5
PI-60/40	14	**60/40**	30	1.5
PI-60 s	14	70/30	**60**	1.5
PI-16%-60/40	**16**	**60/40**	30	1.5

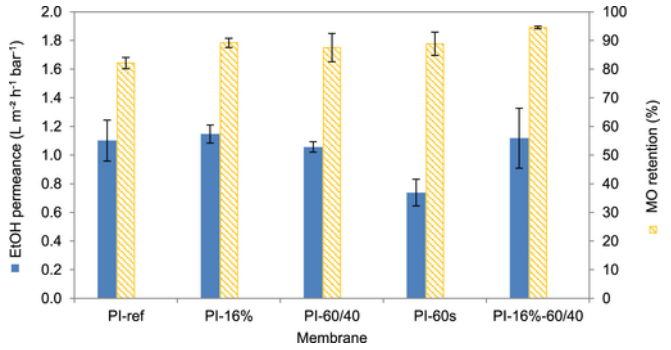

Fig. 10. EtOH permeance and MO retention of denser, cross-linked PI membranes (with low cross-linking degree) prepared via phase inversion, followed by a DMF treatment.

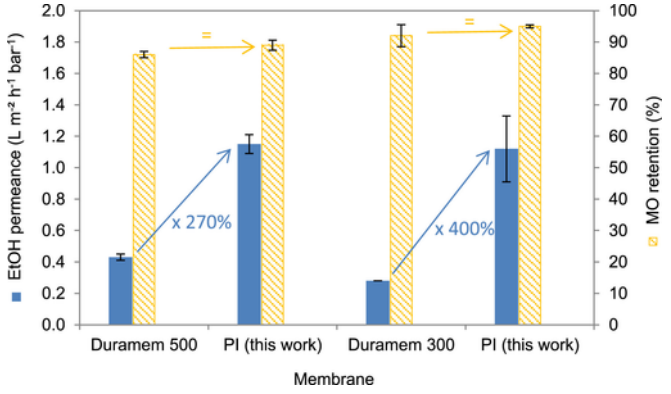

Fig. 11. Comparison of the EtOH permeance and MO retention of commercial Duramem membranes and solvent treated cross-linked PI membranes prepared in this work.

a drastically higher EtOH permeance compared to commercial Duramem membranes with equal selectivity.

Even compared to lab-made TFC polyamide membranes [19], which generally reach higher permeances than ISA membranes, these densified crosslinked PI membranes showed a 180% higher EtOH permeance (0.61 for the TFC membrane compared to 1.12 L m^{-2} h^{-1} bar^{-1} for the PI membrane) with similar selectivity (99% RB (1017 Da) and 96% Sudan Black B (457 Da) retention for the TFC membrane compared to 95% MO (327 Da) retention for the PI membrane).

4. Conclusions

A new, simple method to form highly permeable ISA SRNF membranes was presented, in which a solvent treatment allowed cross-linked PI UF membranes, prepared via phase inversion, to be transformed into NF membranes. The link between the degree of swelling, weight loss of the membranes after immersion in different solvents, Hansen solubility parameters and the effect of the solvent treatment on membrane performance proved that membrane-solvent interactions and swelling were determining factors in the membrane densification. The increased polymer chain flexibility during immersion in a good solvent (i.e. DMF) caused densification and improved chain stacking, by establishing favorable interactions (e.g. hydrogen bonds and π interactions) and increasing the cross-linking degree. Furthermore, the immersion time in the organic solvent and the initial degree of cross-linking of the membrane also influenced the extent of densification.

By changing the PI concentration, the NMP/THF ratio in the polymer solution and the evaporation time between casting and phase inversion of the initial membranes, the performance of the solvent treated membranes could be further tuned. The best performing densified membranes from this work with selectivity equal to Duramem 500 or Duramem 300, reached a respectively 270 or 400% higher EtOH permeance compared to these commercial membranes. Compared to lab-made TFC polyamide membranes [19], solvent treated membranes from this work with similar selectivity showed a 180% higher EtOH permeance. This very simple treatment of existing membranes thus shows a huge potential for SRNF applications, since it enables the formation of highly selective SRNF membranes with exceedingly high EtOH permeance compared to commercial membranes.

Acknowledgements

This work was supported by KU Leuven [OT (11/061) funding and Hercules AKUL/13/19 project] and the Belgian Federal Government [I.A.P. – P.A.I. grant (IAP 7/05 FS2)]. We also wish to thank A. Vandoren from the Laboratory for Entomology of KU Leuven for sample preparation for TEM, C. Van Goethem from the Centre of Surface Chemistry and Catalysis for performing the TEM measurements, and A. Volodin from the Laboratory of Solid-State Physics and Magnetism of KU Leuven for the AFM measurements. We would also like to thank the Heinz Maier-Leibnitz Zentrum for the PLEPS measurements and T. Koschine and R. Verbeke for the evaluation of the PLEPS results.

Appendix A. Supporting information

Supplementary data associated with this article can be found in the online version at doi:10.1016/j.memsci.2017.06.080.

References

[1] M.M. Pendergast, E.M.V. Hoek, A review of water treatment membrane nanotechnologies, Energy Environ. Sci. 4 (2011) 1946–1971, http://dx.doi.org/10.1039/C0EE00541J.

[2] A.W. Mohammad, Y.H. Teow, W.L. Ang, Y.T. Chung, D.L. Oatley-Radcliffe, N. Hilal, Nanofiltration membranes review: recent advances and future prospects, Desalination 356 (2015) 226–254, http://dx.doi.org/10.1016/j.desal.2014.10.043.

[3] A.I. Schäfer, A.G. Fane, T.D. Waite, Nanofiltration: Principles and Applications, Elsevier Advanced Technology, 2005 http://books.google.be/books?id=FspTAAAAMAAJ.

[4] P. Vandezande, L.E.M. Gevers, I.F.J. Vankelecom, Solvent resistant nanofiltration: separating on a molecular level, Chem. Soc. Rev. 37 (2008) 365–405, http://dx.doi.org/10.1039/B610848M.

[5] P. Marchetti, M.F. Jimenez Solomon, G. Szekely, A.G. Livingston, Molecular separation with organic solvent nanofiltration: a critical review, Chem. Rev. 114 (2014) 10735–10806, http://dx.doi.org/10.1021/cr500006j.

[6] G. Szekely, M.F. Jimenez-Solomon, P. Marchetti, J.F. Kim, A.G. Livingston, Sustainability assessment of organic solvent nanofiltration: from fabrication to application, Green Chem. 16 (2014) 4440–4473, http://dx.doi.org/10.1039/C4GC00701H.

[7] S. Adler, E. Beaver, P. Bryan, S. Robinson, J. Watson, Vision 2020: 2000 separations roadmap, Center for Waste Reduction Technologies of the AIChE and Dept. of Energy of the United States of America, 2000.

[8] K. Vanherck, P. Vandezande, S.O. Aldea, I.F.J. Vankelecom, Cross-linked polyimide membranes for solvent resistant nanofiltration in aprotic solvents, J. Membr. Sci. 320 (2008) 468–476, http://dx.doi.org/10.1016/j.memsci.2008.04.026.

[9] K. Hendrix, M. Van Eynde, G. Koeckelberghs, I.F.J. Vankelecom, Crosslinking of modified poly(ether ether ketone) membranes for use in solvent resistant nanofiltration, J. Membr. Sci. 447 (2013) 212–221, http://dx.doi.org/10.1016/j.memsci.2013.07.002.

[10] I.B. Valtcheva, S.C. Kumbharkar, J.F. Kim, Y. Bhole, A.G. Livingston, Beyond polyimide: crosslinked polybenzimidazole membranes for organic solvent nanofiltration (OSN) in harsh environments, J. Membr. Sci. 457 (2014) 62–72, http://dx.doi.org/10.1016/j.memsci.2013.12.069.

[11] I. Struzynska-Piron, J. Loccufier, L. Vanmaele, I.F.J. Vankelecom, Synthesis of solvent stable polymeric membranes via UV depth-curing, Chem. Commun. 49 (2013) 11494–11496, http://dx.doi.org/10.1039/C3CC46795C.

[12] M.F. Jimenez Solomon, Y. Bhole, A.G. Livingston, High flux membranes for organic solvent nanofiltration (OSN) – interfacial polymerization with solvent activation, J. Membr. Sci. 423–424 (2012) 371–382, http://dx.doi.org/10.1016/j.memsci.2012.08.030.

[13] S. Hermans, E. Dom, H. Mariën, G. Koeckelberghs, I.F.J. Vankelecom, Efficient synthesis of interfacially polymerized membranes for solvent resistant nanofiltration, J. Membr. Sci. 476 (2015) 356–363, http://dx.doi.org/10.1016/j.memsci.2014.11.046.

[14] S. Hermans, H. Mariën, C. Van Goethem, I.F. Vankelecom, Recent developments in thin film (nano)composite membranes for solvent resistant nanofiltration, Curr. Opin. Chem. Eng. 8 (2015) 45–54, http://dx.doi.org/10.1016/j.coche.2015.01.009.

[15] J. Aburabie, P. Neelakanda, M. Karunakaran, K.-V. Peinemann, Thin-film composite crosslinked polythiosemicarbazide membranes for organic solvent nanofiltration (OSN), React. Funct. Polym. 86 (2015) 225–232, http://dx.doi.org/10.1016/j.reactfunctpolym.2014.09.011.

[16] L. Pérez-Manríquez, J. Aburabi'e, P. Neelakanda, K.-V. Peinemann, Cross-linked PAN-based thin-film composite membranes for non-aqueous nanofiltration, React. Funct. Polym. 86 (2015) 243–247, http://dx.doi.org/10.1016/j.reactfunctpolym.2014.09.015.

[17] J.R. Werber, C.O. Osuji, M. Elimelech, Materials for next-generation desalination and water purification membranes, Nat. Rev. Mater. 1 (2016) 16018.

[18] M.F. Jimenez Solomon, Y. Bhole, A.G. Livingston, High flux hydrophobic membranes for organic solvent nanofiltration (OSN) – interfacial polymerization, surface modification and solvent activation, J. Membr. Sci. 434 (2013) 193–203, http://dx.doi.org/10.1016/j.memsci.2013.01.055.

[19] H. Mariën, L. Bellings, S. Hermans, I.F.J. Vankelecom, Sustainable process for the preparation of high-performance thin-film composite membranes using ionic liquids as the reaction medium, ChemSusChem 9 (2016) 1101–1111, http://dx.doi.org/10.1002/cssc.201600123.

[20] K. Vanherck, A. Cano-Odena, G. Koeckelberghs, T. Dedroog, I. Vankelecom, A simplified diamine crosslinking method for PI nanofiltration membranes, J. Membr. Sci. 353 (2010) 135–143, http://dx.doi.org/10.1016/j.memsci.2010.02.046.

[21] K. Vanherck, G. Koeckelberghs, I.F.J. Vankelecom, Crosslinking polyimides for membrane applications: a review, Prog. Polym. Sci. 38 (2013) 874–896, http://dx.doi.org/10.1016/j.progpolymsci.2012.11.001.

[22] P. Vandezande, L.E.M. Gevers, J.S. Paul, I.F.J. Vankelecom, P.A. Jacobs, High throughput screening for rapid development of membranes and membrane processes, J. Membr. Sci. 250 (2005) 305–310, http://dx.doi.org/10.1016/j.memsci.2004.11.002.

[23] I. Horcas, R. Fernández, J.M. Gómez-Rodríguez, J. Colchero, J. Gómez-Herrero, A.M. Baro, WSXM: a software for scanning probe microscopy and a tool for nanotechnology, Rev. Sci. Instrum. 78 (2007) http://dx.doi.org/10.1063/1.2432410.

[24] S.J. Tao, Positronium annihilation in molecular substances, J. Chem. Phys. 56 (1972) 5499–5510, http://dx.doi.org/10.1063/1.1677067.

[25] M. Eldrup, D. Lightbody, J.N. Sherwood, The temperature dependence of positron lifetimes in solid pivalic acid, Chem. Phys. 63 (1981) 51–58, http://dx.doi.org/10.1016/0301-0104(81)80307-2.

[26] C.M. Hansen, Hansen Solubility Parameters: A User's Handbook, Second edition, CRC Press, 2007 https://books.google.be/books?id=gprF31cvT2oC.

[27] I.-C. Kim, H.-G. Yun, K.-H. Lee, Preparation of asymmetric polyacrylonitrile membrane with small pore size by phase inversion and post-treatment process, J. Membr. Sci. 199 (2002) 75–84, http://dx.doi.org/10.1016/S0376-7388(01)00680-9.

[28] Y.H. See-Toh, F.C. Ferreira, A.G. Livingston, The influence of membrane formation parameters on the functional performance of organic solvent nanofiltration membranes, J. Membr. Sci. 299 (2007) 236–250, http://dx.doi.org/10.1016/j.memsci.2007.04.047.

[29] A. Cano-Odena, M. Spilliers, T. Dedroog, K. De Grave, J. Ramon, I.F.J. Vankelecom, Optimization of cellulose acetate nanofiltration membranes for micropollutant removal via genetic algorithms and high throughput experimentation, J. Membr. Sci. 366 (2011) 25–32, http://dx.doi.org/10.1016/j.memsci.2010.09.026.

[30] S. Basu, A.L. Khan, A. Cano-Odena, C. Liu, I.F.J. Vankelecom, Membrane-based technologies for biogas separations, Chem. Soc. Rev. 39 (2010) 750–768, http://dx.doi.org/10.1039/B817050A.

[31] J.J. Krol, M. Boerrigter, G.H. Koops, Polyimide hollow fiber gas separation membranes: preparation and the suppression of plasticization in propane/propylene environments, J. Membr. Sci. 184 (2001) 275–286, http://dx.doi.org/10.1016/S0376-7388(00)00640-2.

[32] J. da Silva Burgal, L. Peeva, A. Livingston, Negligible ageing in poly(ether-ether-ketone) membranes widens application range for solvent processing, J. Membr. Sci. 525 (2017) 48–56, http://dx.doi.org/10.1016/j.memsci.2016.10.015.

[33] P. Kubisa, Ionic liquids as solvents for polymerization processes – progress and challenges, Prog. Polym. Sci. 34 (2009) 1333–1347, http://dx.doi.org/10.1016/j.progpolymsci.2009.09.001.

[34] N. Winterton, Solubilization of polymers by ionic liquids, J. Mater. Chem. 16 (2006) 4281–4293, http://dx.doi.org/10.1039/B610143G.

[35] S. Livazovic, Z. Li, A.R. Behzad, K.-V. Peinemann, S.P. Nunes, Cellulose multilayer membranes manufacture with ionic liquid, J. Membr. Sci. 490 (2015) 282–293, http://dx.doi.org/10.1016/j.memsci.2015.05.009.

[36] D.Y. Xing, S.Y. Chan, T.-S. Chung, The ionic liquid [EMIM]OAc as a solvent to fabricate stable polybenzimidazole membranes for organic solvent nanofiltration, Green Chem. 16 (2014) 1383–1392, http://dx.doi.org/10.1039/C3GC41634H.

[37] K.-S. Liao, H. Chen, S. Awad, J.-P. Yuan, W.-S. Hung, K.-R. Lee, J.-Y. Lai, C.-C. Hu, Y.C. Jean, Determination of free-volume properties in polymers without orthopositronium components in positron annihilation lifetime spectroscopy, Macromolecules 44 (2011) 6818–6826, http://dx.doi.org/10.1021/ma201324k.

[38] L.K. Wang, J.P. Chen, Y.T. Hung, N.K. Shammas, Membrane and Desalination Technologies, Springer, New York, 2010 https://books.google.be/books?id=CMOBQ8ijJbwC.

[39] A.K. Hołda, B. Aernouts, W. Saeys, I.F.J. Vankelecom, Study of polymer concentration and evaporation time as phase inversion parameters for polysulfone-based SRNF membranes, J. Membr. Sci, 442, 2013196–205, http://dx.doi.org/10.1016/j.memsci.2013.04.017.

[40] P. Vandezande, X. Li, L.E.M. Gevers, I.F.J. Vankelecom, High throughput study of phase inversion parameters for polyimide-based SRNF membranes, J. Membr. Sci. 330 (2009) 307–318, http://dx.doi.org/10.1016/j.memsci.2008.12.068.